Int. J. Exp. Path. (2005), 86, 45–55

ORIGINAL ARTICLE

Ultrastructural evaluation of the radioprotective effects of melatonin against X-ray-induced skin damage in Albino rats

Mahmoud R. Hussein[*], Eman E. Abu-Dief[†], Mohammad H. Abd el-Reheem[†] and Ali Abd-Elrahman[‡]

[*]*Department of Pathology, Faculty of Medicine, Assuit University, Assuit, Egypt, and Departments of* [†]*Histology and* [‡]*Clinical Oncology, Faculty of Medicine, South Valley University, Sohag, Egypt*

INTERNATIONAL JOURNAL OF EXPERIMENTAL PATHOLOGY

Summary

Our knowledge about the radioprotective effects of melatonin against X-ray-induced skin damage is still lacking. To examine these effects, an animal model of 60 Albino rats was used. The animals were divided into five groups: Group 1, nonirradiated; Group 2, X-ray irradiated (XRI, 8 Gy); Group 3, XRI pretreated with solvent (ethanol and phosphate-buffered saline); Group 4, nonirradiated group treated with melatonin; and Group 5, XRI pretreated with melatonin. The skin was evaluated for ultrastructural changes using transmission electron microscopy (TEM). When compared to the nonirradiated skin (Groups 1 and 4), XRI skin (Groups 2 and 3) showed features of both cell injury and increased metabolic activity. The former included changes such as condensation of the nuclei, vacuolization of the cytoplasm, dilatation of the rough endoplasmic reticulum, swelling of the mitochondria with cristolysis, destruction of the ribosomes and intermediate filaments, fragmentation of the keratohyaline granules and loss of the irregularity of the basal cell borders. The central cells of the sebaceous gland alveoli had larger irregular nuclei and few lipid droplets in their cytoplasm. The hair follicle cells had heterochromatic nuclei and less electron dense cytoplasm containing few complements of the organelles. The features of increased metabolic activity included increased euchromatin, irregularity of the nuclear membrane and increased branching of the melanocytes. Also, an increased number of the Birbeck granules were seen in the Langerhans cells. When compared to the irradiated skin (Groups 2 and 3), these changes were mild or absent in the skin of XRI animals pretreated with melatonin (Group 5). The ability of melatonin to minimize the injurious effects of XRI suggests a radioprotective role. The clinical ramifications of these observations warrant further studies.

Keywords
Skin, melatonin, X-ray irradiation

Received for publication:
18 June 2004
Accepted for publication:
13 October 2004

Correspondence:
Mahmoud R. Hussein MSc, MD, PhD
Department of Pathology
Faculty of Medicine
Assuit University
Assuit, Egypt
Tel.: +88 93 583 166
Fax: +88 33 272 727
E-mail: mrh17@swissinfo.org

Introduction

The X-rays (electromagnetic ionizing radiation) are composed of massless particles of energy (photons) that disrupt the electrons of atoms within cells and therefore affect cellular functions. X-ray irradiation (XRI) can affect both normal and neoplastic cells especially the rapidly growing ones such as the epidermal cells. Although X-rays are widely used for both imaging and therapeutic purposes, our knowledge about their possible injurious effects on the skin is incomplete. Clinically, XRI can produce erythema as well as dry and moist desquamation. Morphologically, XRI can produce epidermal loss, cristolysis, cytoplasmic vacuolization, appearance of euchromatic nuclei, altered microvasculature, hyperkeratinization, redistribution of biometals, as well as basal and squamous cell carcinoma. The type and extent of these changes depends on the dose, duration and frequency of XRI (Berry *et al*. 1976; Archambeau *et al*. 1984; Enokihara *et al*. 1993; De Chatterjee *et al*. 1994; Landthaler *et al*. 1995; Shore *et al*. 2002).

Melatonin is a secretory product of the pineal gland. It can participate in the regulation of numbers of physiological and pathological processes. It can scavenge many harmful free radicals such as hydroxyl, peroxyl radicals and peroxynitrite anions. Melatonin accumulates more in the nucleus than in the cytosol of the cell. Also, it is one of the few antioxidants that can penetrate the mitochondrial membrane and enter the mitochondria. Therefore, it has a radioprotective role. In support of this proposition, melatonin can: (1) improve the overall survival following total body irradiation, and (2) minimize the extent of DNA damage and the frequency of chromosomal abrasions (Hickman *et al*. 1999; Vijayalaxmi *et al*. 1999a).

To date, the radioprotective role of melatonin against X-ray-induced skin damage is still unknown. In this investigation, we hypothesized that melatonin can minimize the cell injury associated with XRI. This radioprotective effect would manifest on the ultrastructural level by preservation of the nuclear and cytoplasmic features. To test our hypothesis and to fill this existing gap in the literature, we carried out this investigation. To accomplish our goals, we established an animal model consisting of five groups of Albino rats: (1) non-XRI, (2) XRI, (3) XRI-pretreated with solvent, (4) non-XRI pretreated with melatonin and (5) XRI pretreated with melatonin. We addressed two questions: (1) what are the morphological changes in XRI skin? and (2) what are the effects of melatonin on these morphological changes?

Materials and methods

The experimental protocol was approved by the Institutional Animal Care and Use Committee of the South Valley University, School of Medicine, Sohag, Egypt.

Rats and maintenance

Three-month old Albino rats were obtained from Assuit University Animal Facility, Faculty of Medicine, Assuit University, Assuit, Egypt. They were housed in Animal facility, Faculty of medicine, South Valley University, Sohag, Egypt, with room temperature maintained at 65–75 °F, relative humidity of 50–70% and an airflow rate of 15 exchange/h. Also, a time-controlled system provided 07:00–21:00 hours of light and 21:00–07:00 hours of dark cycles. All rats were given *ad libitum* access to Taklad rodent chow diet and water from sanitized bottle fitted with stopper and sipper tubes. These conditions were adopted following other groups (Vijayalaxmi *et al*. 1999a, b).

Melatonin and X-ray irradiation

After a 7-day acclimatization period, a randomized block design based on the animal body weights was used to divide the rats into five different groups. Five separate experiments were executed using a total of 60 rats. Each experiment had 12 rats in each of the following groups: Group 1, non-XRI; Group 2, XRI (8 Gy whole body); Group 3, XRI-pretreated with solvent (5% ethanol in phosphate buffer saline 1 h before irradiation); Group 4, intraperitoneal injection of melatonin (100 mg/kg body weight); and Group 5, XRI-pretreated with melatonin (100 mg/kg body weight melatonin 1 h before irradiation). The animals in Groups 1, 3 and 4 served as controls for experimental animals in Groups 2 and 5. The irradiation was carried out using Gs Gamma irradiators. Animals in Groups 2, 3 and 5 were exposed to a whole body XRI dose of 8 Gy. Animals in Groups 4 and 5 were given an intraperitoneal injection of freshly prepared melatonin (Sigma, St. Louis, MO, USA) in 100 µl of 5% ethanol (made with phosphate-buffered saline). Following other groups, we selected this XRI-specific dose as it can generate reactive oxygen radicles, induce apoptosis, and alter in the cell-cycle protein expression in cultured skin fibroblast (Kim *et al*. 2001 and Sener *et al*. 2003).

Histological examination of the specimens

All the animals were scarified at 48 h after XRI. Several skin tissue pieces were obtained from the ear pinnae of each animal. Some of these tissues were formalin-fixed, paraffin-embedded and processed for the routine histology. Others were processed for ultrastructural studies.

Transmission electron microscopy (TEM)

Some tissue fragments were fixed in 2.5% in 0.1 M sodium cacodylate buffer at 40 °C and pH 7.2 for 24 h, washed in

0.1 M buffer, post fixed in osmium tetroxide in 0.2 M buffer for 1 h. The specimens were dehydrated in 70, 90 and 100% ethanol and then embedded in labelled capsules with freshly prepared resin and left to polymerize at 60 °C for 48 h. Several resin semithin sections were cut at approximately 1 μm using glass knives and an ultramicrotome. The sections were stained with 1% toluidine blue in 1% borax solution for 1 min at 80 °C. The stain was rinsed off with distilled water, and the sections were dried and examined. Selective areas from the trimmed blocks were cut by using a diamond knife, with the ultramicrotome set to cut at around 50–70 nm using heat advances. The sections were picked up onto 300-mesh copper grids, stained with methanolic uranyl acetate and examined by TEM. Some of the examined fields were photographed (Hussein *et al.* 2003c).

Examination of morphological changes

The routine (hematoxylin and eosin) stained sections were examined. The tissues were then processed for evaluation with TEM as previously described (Hussein *et al.* 2003c). Histological evaluation of apoptosis followed the established criteria reported in the original paper by Kerr and colleagues (Hussein *et al.* 2003a, b). These criteria include condensed nuclear fragments, nuclei with marginated chromatin, multiple nuclear fragments, a single condensed nucleus, membrane-bound structures containing variable amounts of chromatin and/or cytoplasm and eosinophilic cytoplasm. Quantification of the features of cell damage was (some organelles and granules) done by counting them in 20 random TEMs with final magnification of ×10,000. The results were expressed as mean and standard error of mean (Mean ± SEM).

Statistical analysis

Analysis of variance (ANOVA) with a statistical significance of $P < 0.05$, was used (Statistix for Windows 1985, 1996; Analytical Software Program).

Results

Ultrastructural features of the non-XRI skin (Groups 1 and 4)

The epidermis was formed of one (basal), two (spinous and granular, each) layers and some layers of squamous corneocytes. The basal cells were columnar in shape with elongated euchromatic nuclei and inconspicuous nucleoli. The cytoplasm contained numerous mitochondria, ribosomes, and moderate amounts of intermediate filaments (IF) in the form of bundles especially at the periphery of the cells. Some profiles of rough endoplasmic reticulum (RER) and small Golgi saccules were seen. The basal borders of the cells were irregular, attached to the underlying basement membrane with numerous hemidesmosomes. The lateral and apical borders of the cells were attached to the surrounding cells by numerous desmosomes (Figure 1a). The spinous cells were polyhedral with rounded slightly indented euchromatic nuclei. The cytoplasm contained

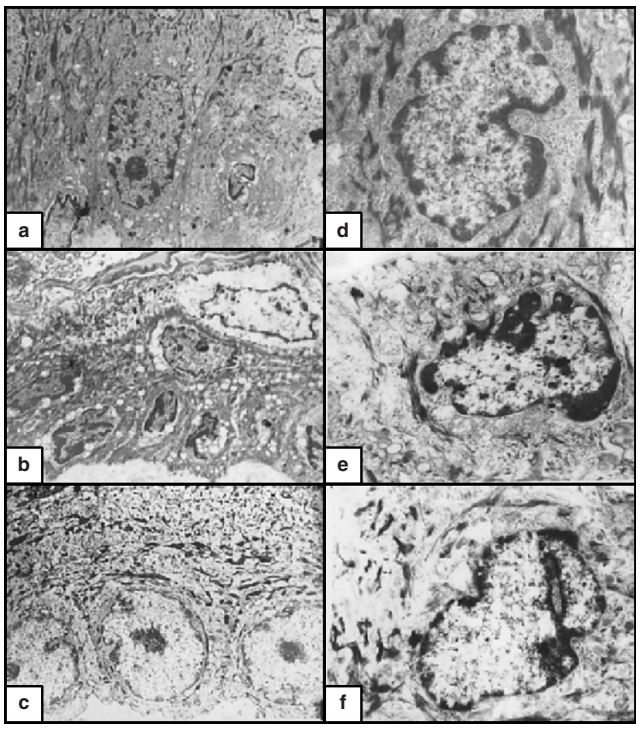

Figure 1 (a) Non-irradiated skin. The basal cells had euchromatic nuclei and conspicuous nucleoli. The cytoplasm contained full complements of organelles. The basal borders of the cells were irregular (×4000). (b) X-ray-irradiated skin. The basal cells were relatively small with small-condensed, irregular heterochromatic nuclei. The cytoplasm contained numerous vacuoles representing swollen mitochondria and dilated RER. The irregularity of the basal borders were markedly lost (×4000). (c) X-ray-irradiated skin pretreated with melatonin. The basal cells were large with euchromatic nuclei. The cytoplasm contained almost similar numbers of organelles as compared to the nonirradiated group. There was mild loss in the irregularity of the basal membrane (×4000). (d) Non-irradiated skin. The spinous cells were polyhedral with euchromatic nuclei. The cytoplasm contained full complements of organelles. The lateral borders of the cells had numerous desmosomes (×15,000). (e) X-ray-irradiated skin. The spinous cells were polyhedral with small heterochromatic nuclei. The cytoplasm contained numerous vacuoles and few organelles. The lateral borders of the cells had few desmosomes (×10,000). (f) X-ray-irradiated skin pretreated with melatonin. The spinous cells were polyhedral, with euchromatic nuclei. The cytoplasm contained slightly fewer numbers of organelles as compared to nonirradiated cells. The lateral borders of the cells had numerous desmosomes (×10,000).

complements of organelles similar to those of the basal cells together with some membrane-bounded granules (MG) (Figure 1d). The lateral borders of the cells were attached to the surrounding cells by numerous desmosomes. The granular cells appeared as elongated slightly flat cells with flat nuclei. The latter were usually masked by electron dark nonmembranous granules (NMG). The corneocytes were squamous cells with thick plasma membranes (Figure 2a).

The melanocytes were occasionally seen among the basal keratinocytes. They appeared as small, oval cells with short branches, convoluted nuclei and prominent nucleoli. The cytoplasm contained small Golgi, some profiles of RER and few melanosomes (Figure 3d). Langerhans cells appeared as large, rounded cells. They were found among spinous cells without any desmosomes joining them. Their nuclei were highly convoluted and their cytoplasm contained moderate amounts of Golgi, some profiles of RER and some Birbecks granules (Figure 3a).

The sebaceous gland alveolus (SGA) consisted of peripheral and central differentiating and highly differentiated cells. The former type were an oval cells containing abundant smooth and RER, free ribosomes, mitochondria, small Golgi, some

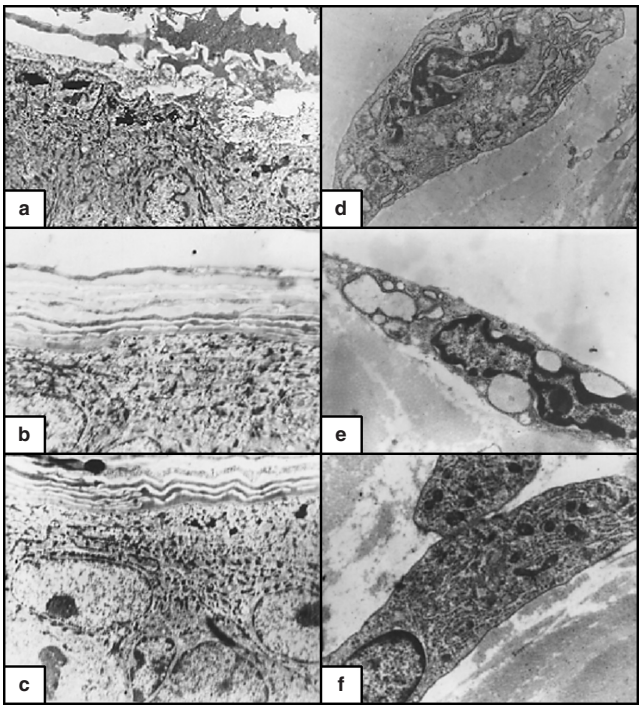

Figure 2 (a) Non-irradiated skin. The granular cells were elongated, slightly flattened with flattened nuclei, masked by electron dark nonmembranous granules (NMG). The corneocytes were squamous cells with thick plasma membranes (×4000). (b) X-ray-irradiated skin. The granular cells were flattened, contained small, few NMG and fragmented keratohyaline granules. The corneocytes were squamous cells with very irregular outlines (×4000). (c) X-ray-irradiated skin pretreated with melatonin. The granular layer contained considerable numbers of NMG with mild fragmentation of the keratohyaline granules. The corneocytes had similar appearance to those of the nonirradiated group (×4000). (d) Non-irradiated skin. The fibroblasts were elongated; branched cells with elongated heterochromatic nuclei. The cytoplasm contained well-developed Golgi, RER cisternae and some mitochondria (×10,000). (e) X-ray-irradiated skin. The fibroblasts were relatively small in size, with more heterochromatic nuclei, ballooning of Golgi saccules and RER cisternae (×10,000). (f) X-ray-irradiated skin pretreated with melatonin. The fibroblasts had euchromatic nuclei. The cytoplasm contained full complement of organelles (×10,000).

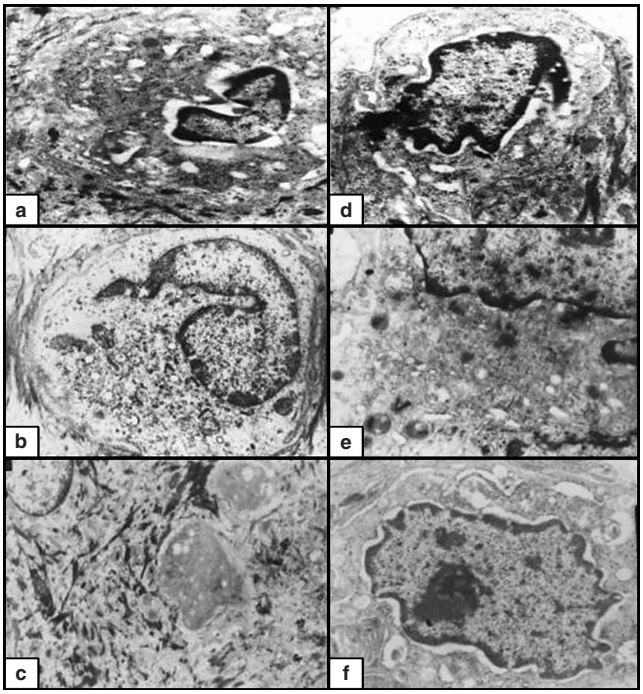

Figure 3 (a) Non-irradiated skin. Langerhans cells were large, rounded, with highly convoluted nuclei. The cytoplasm contained moderate profile of organelles and some Birbecks granules (×12,000). (b) X-ray-irradiated skin. Langerhans cells were relatively large with more numerous Birbecks granules and less electron-dense cytoplasm (×12000). (c) X-ray-irradiated skin pretreated with melatonin. Langerhans cells were more frequent and had similar features as the nonirradiated group (×6000). (d) Non-irradiated skin. The melanocytes appeared as small oval cells with short and few branches, convoluted nuclei and prominent nucleoli. The cytoplasm contained small Golgi, some profiles of RER and few melanosomes (×12,000). (e) X-ray-irradiated skin. The melanocytes appeared as large cells. Their cytoplasm contained numerous cisternae of RER, Golgi saccules and melanosomes at different stages of maturation (X12000). (f) X-ray irradiated skin pretreated with melatonin. The melanocytes appeared as slightly large cells. Their cytoplasm contained moderate sized Golgi, RER and some melanosomes (×12,000).

glycogen particles, intermediate filaments (IM) filaments and few lipid droplets. The cells towards the centre had irregular nuclei with inconspicuous nucleoli and large lipid droplets, which compress the cellular remnants into thin strands (Figure 4a). The cells of the hair follicle were rounded with irregular borders. They were joined together by numerous desmosomes. Their nuclei were rounded and euchromatic with prominent nucleoli. The cytoplasm contained numerous mitochondria, ribosomes, IF and some profiles of ER (Figure 4d). The fibroblasts of the control group appeared as elongated cells with elongated euchromatic nuclei and inconspicuous nucleoli. The cytoplasm contained well-developed Golgi, RER cisternae and some mitochondria (Figure 2d). The endothelial cells were overlapping and had euchromatic nuclei (Figure 5a, Tables 1–3).

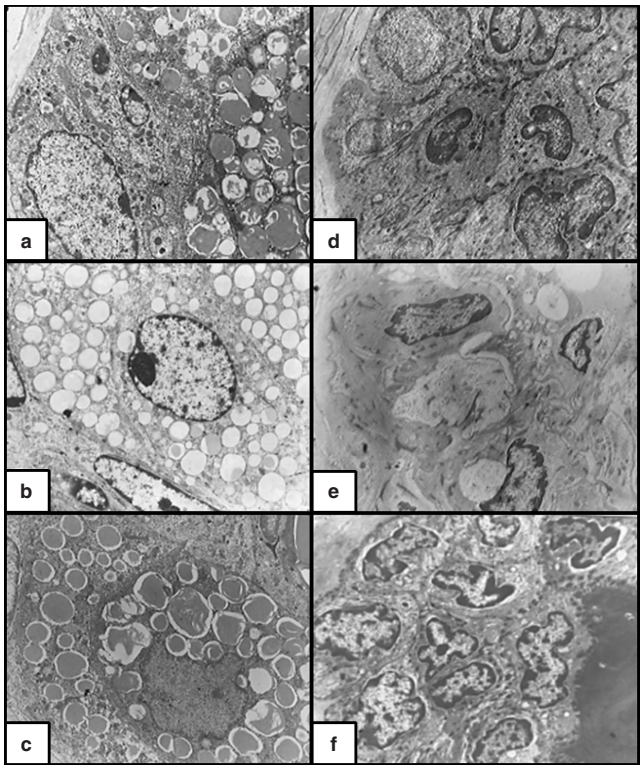

Figure 4 (a) Non-irradiated skin. The sebaceous gland alveolus (SGA) consisted of basal cell, differentiating cells and a part of well-differentiated central cell full of lipid droplets, electron dense (×4000). (b) X-ray-irradiated skin. The SGA consisted of basal cells, differentiating cells and a part of a central cell. The lipid droplets are smaller in size and less electron dense as compared to the nonirradiated group (×4000). (c) X-ray-irradiated skin pretreated with melatonin. The SGA central cells contained a considerable number of lipid droplets, which were electron dense and similar to those of the nonirradiated group. (d) Non-irradiated skin. The cells of the hair follicle had euchromatic nuclei, numerous desmosomes, and electron-dense cytoplasm. The cytoplasm contained numerous mitochondria, ribosomes, IF and some profiles of RER (×4000). (e) X-ray-irradiated skin. The cells of the hair follicle had heterochromatic nuclei and less electron-dense cytoplasm containing few complements of organelles. There was marked widening of the intercellular spaces with few desmosomes joining the adjacent cells together (×4000). (f) X-ray-irradiated skin pretreated with melatonin. The cells of the hair follicle were almost similar to those of the nonirradiated group with numerous desmosomes joining them together (×4000).

Ultrastructural features of the XRI skin (Groups 2 and 3)

As compared to the nonirradiated skin, the XRI skin had several features indicative of both cell injury and increased metabolic activity. The stratification of the epidermis was reduced to one layer each of basal, spinous and granular cells as well as few layers of corneocytes. The cells of the basal layer were relatively small in size with small-condensed nuclei. The

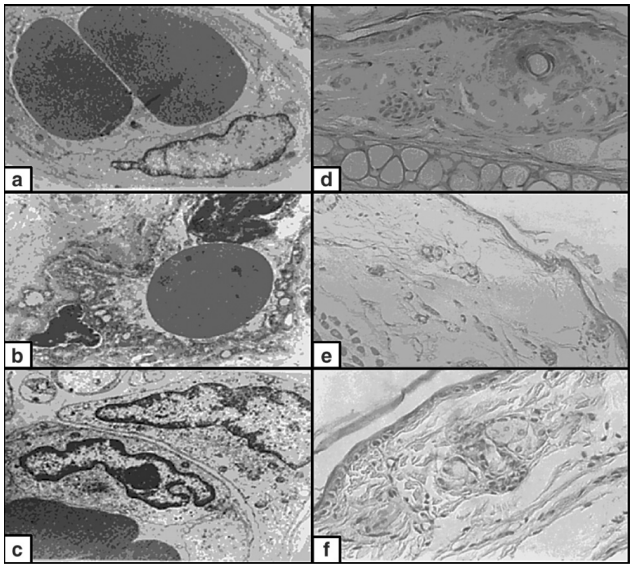

Figure 5 (a) Non-irradiated skin. The endothelial lining cells with euchromatic nuclei, desmosomes between them with some overlapping (×8000). (b) X-ray-irradiated skin. The endothelial cells with marked irregular surfaces, heterochromatic irregular nuclei, numerous pinocytotic vesicles and marked widening of the intercellular spaces (×8000). (c) X-ray-irradiated skin pretreated with melatonin. The endothelial cells had slightly heterochromatic nuclei and minimal widening of the intercellular spaces (×8000). (d) Non-irradiated skin. The epidermis is formed of one basal, two spinous and one granular cell layers (×400). (e) X-ray-irradiated skin. The epidermis is formed of basal, spinous and granular cell layers (one layer each). Marked oedema of the dermis and disruption of the dermal connective tissue (×400). (f) X-ray-irradiated skin pretreated with melatonin. The epidermis was formed of one basal, two spinous and one granular layers. The dermal connective tissue is similar to the nonirradiated group (×400).

Table 1 Ultrastructural changes in the skin of irradiated and irradiated melatonin pretreated animals

Aspect	X-ray-irradiated skin	X-ray-irradiated skin with melatonin pretreatment
Basal and spinous cells		
Nuclei	The nuclei were more condensed with markedly irregular contour (indentations), more euchromatin and marginal chromatin masses	The nuclei were less condensed, mildly irregular contour, more hetrochromatin, less marginal chromatin masses
Nucleoli	The nucleoli were inconspicuous	The nucleoli were conspicuous and regular in shape
Cytoplasmic organelles	The mitochondria were swollen with cistolysis. The RER were dilated. The ribosomes, MG, IF, NMG markedly decreased in numbers. Frequent cytoplasmic vacuolization. No apoptotic bodies. Marked loss of the irregularity of the basal borders of the basal cells	The mitochondria and RER, ribosomes, MG, IF, NMG were almost similar to the nonirradiated cells. No cytoplasmic vacuolization or apoptotic bodies. Mild loss borders of basal cells of the irregularity
Granular cell layer	Marked fragmentation of the keratohyaline. The cytoplasm had less electron-dense cytoplasm. The corneocytes lost their irregular borders.	Mild fragmentation of the keratohyaline granules. The cytoplasm is more electron dense. The corneocytes had irregular borders
Melanocytes	Large, more branched, with numerous RER, and melanosomes at different stages of differentiation	Small, less branched, with few complements of RER, Golgi and melanosomes
Langerhans cells	Large, with abundant Birbecks granules	Large with few Birbecks granules
Sebaceous glands	The central cells were not degenerated. The nuclei of the central and germinative cells were condensed with prominent nucleoli and decreased lipid droplets	The central cells were degenerated. The nuclei of the central and germinative cells were similar to those of nonirradiated skin
Fibroblasts	Large, more branched, heterochromatic nuclei, ballooning of Golgi and RER	Small, less branched, euchromatic nuclei. No ballooning of Golgi and RER
Hair follicle cells	Heterochromatic nuclei. The cytoplasm is less electron dense, with marked widening of the intercellular spaces, with few desmosomes	Euchromatic nuclei. The cytoplasm is more electron dense, without widening of the intercellular spaces. Numerous desmosomes
Endothelial cells	Marked irregularity of their surfaces, hetrochromatic irregular nuclei, numerous pinocytotic vesicles, more widening of the intercellular spaces with rare desmosomes	No irregularity of their surfaces, euchromatic regular nuclei, no pinocytotic vesicles, less widening of the intercellular spaces with more desmosomes

IF, intermediate filaments; MG, membrane bound granules; NMG, nonmembrane bound granules; RER, rough endoplasmic reticulum.

nuclear membranes of the cells were markedly irregular due to the presence of numerous indentations. There was an increase in the amount of the euchromatin with its margination. The nucleoli were conspicuous. The cytoplasm contained numerous vacuoles representing the swollen mitochondria with destructed cristae (cristolysis) and some dilated profiles of RER. The basal borders of these cells were less irregular with less numerous desmosomes (Figure 1b). The spinous cells were polyhedral with small heterochromatic nuclei. The cytoplasm contained numerous vacuoles with less abundant IF, ribosomes and rare MG (Figure 1e). The lateral borders of the cells were attached to the surrounding cells by few desmosomes. The granular cells were flattened, contained small, few NMG. Some of these cells were hypertrophied with large nuclei and vacuolated cytoplasm. The corneocytes were squamous cells with very irregular outlines (Figure 2b). Moreover, the irradiated cells displayed some features of apoptosis such as reduction in the cytoplasmic and nuclear volume, extensive cytoplasmic vacuolization, abnormal ER, mitochondria and condensation of the nuclear chromatin. However, no apoptotic bodies were seen.

The melanocytes were large and highly branched. Their cytoplasm contained numerous cisternae of RER, Golgi saccules and melanosomes at different stages of maturation (Figure 3e). Langerhans cells were relatively large with more

Table 2 Ultrastructural changes in the X-ray-irradiated skin of Albino rats

Features of cell damage	Features of increased metabolic activity	Features of apoptosis
Destruction of the spinous layer	Increased euchromatin	Cytoplasmic vacuolization
Decreased irregularity of the basal cell borders	Irregularity of the nuclear membrane	Reduced nuclear and cytoplasmic areas
Swollen mitochondria and dilated RER cisternae	Margination of the chromatin	Condensation of the nuclear chromatin
Decreased ribosomes, IF,NMG, MG	Prominence of the nucleoli	Abnormal RER
Fragmentation of the keratohyaline granules	Large Langerhans' cells	Abnormal mitochondria
Decrease complement of organelles in the hair follicle	Increased branching of the melanocytes	
Loss of the desmosomes		
Widening of the intercellular spaces		
Depletion of the lipid droplets in SGA		

The ultrastructural features of cellular injury, increased metabolic activity and apoptosis in the X-ray irradiated and X-ray irradiated skin pretreated with melatonin.

numerous Birbecks granules and less electron-dense cytoplasm (Figure 3b). The SGA central cells had large and more irregular nuclei and the cytoplasm contained fewer number of lipid droplets. The latter were less electron dense as compared to the nonirradiated skin (Figure 4b). The cells of the hair follicle (shaft and bulb) had heterochromatic nuclei and less electron-dense cytoplasm with few complements of organelles. There was marked increase in the intercellular spaces with few desmosomes joining the adjacent cells together (Figure 4e). The fibroblasts were relatively small in size and had few branches. Their nuclei were heterochromatic with conspicuous nucleoli. There was a marked dilatation (ballooning) of Golgi saccules and RER cisternae (Figure 2e). The endothelial cells had marked irregularity of their luminal surfaces, heterochromatic irregular nuclei, numerous pinocytotic vesicles and widening of the intercellular spaces (Figure 5b, Tables 1–3).

Ultrastructural features of XRI skin pretreated melatonin (Group 5)

As compared to the XRI skin, the skin pretreated with melatonin prior to XRI had mild or absent changes indicative of cellular damage or increased metabolic activity. The epidermis was formed of one basal, two spinous, and one granular layers as well as some layers of squamous corneocytes. The basal cells were large rounded, with large rounded nuclei, conspicuous nucleoli and large amount of euchromatin. The nuclear membrane was mildly irregular. The cytoplasm contained slightly few numbers of mitochondria, ribosomes and IF as compared to the nonirradiated group (Figure 1c). There was mild decrease in the irregularity of the basal membrane. The spinous cells were large, rounded, polyhedral, with large rounded slightly indented euchromatic nucleus and prominent nucleolus. They contained slightly fewer number of mitochondria and ribosomes but almost similar amounts of IF and MG (Figure 1f). The lateral borders of the cells were attached to the surrounding cells by numerous desmosomes. The granular layer contained considerable numbers of NMG. The corneocytes had similar appearance to those of the nonirradiated group (Figure 2c).

The melanocytes were slightly large in size and branched. Their cytoplasm contained moderate sized Golgi, RER and some melanosomes (Figure 3f). Langerhans cells were more frequent and had a similar structure to the nonirradiated

Table 3 Quantification of the features of cell damage in the skin of Albino rats

Features of cell damage	Non-irradiated skin	X-ray-irradiated skin	XRI skin with melatonin pretreatment	*P*-value
Apoptotic changes	1.2 ± 0.3	5.0 ± 0.7	2.4 ± 0.5	0.001
Cytoplasmic vacoulization	2.2 ± 0.9	8.2 ± 1.3	4 ± 0.9	0.004
Birbecks granules	4.8 ± 0.9	7.6 ± 0.9	4.8 ± 1.1	0.030
Non-swollen mitochondria	6.6 ± 0.9	1.6 ± 0.7	4.4 ± 0.5	0.002
Swollen mitochondria	0.0 ± 0.0	5 ± 0.8	1.8 ± 0.4	0.000
Density of the lipid droplets				
Dense	21 ± 2.3	2.0 ± 0.7	22 ± 1.4	0.000
Less dense	4.4 ± 0.9	22 ± 1.07	2.0 ± 0.7	0.000

P-values refer to XRI *vs*. XRI skin with melatonin pretreatment.

group (Figure 3c). The SGA central cells contained a considerable number of lipid droplets, which were electron dense similar to those demonstrated in nonirradiated group (Figure 4c). The hair follicle cells (shaft and bulb) were almost similar to those of the nonirradiated group but the nuclei were more heterochromatic (Figure 4f). The fibroblasts were more or less similar to those of the nonirradiated group (Figure 2f). The endothelial cells had heterochromatic nuclei and less widened intercellular spaces (Figure 5c, Tables 1 and 2).

Histological evaluation of the skin

The nonirradiated skin was formed of one basal, two spinous and one granular layers (Figure 5d). The XRI skin was formed of basal, spinous and granular (one each) with marked destruction of the dermal connective tissues (Figure 5e). The XRI skin pretreated with melatonin was formed of one basal, two spinous and one granular. The dermal connective tissues were almost similar to the nonirradiated skin (Figure 5f).

Quantification of the features of cell injury and increased metabolic activity

Further quantification of the features of cell injury and increased metabolic activity revealed statistically significant differences between the nonirradiated and X-ray-irradiated skin. A summary of these results was shown in Table 3.

Discussion

Our knowledge about the radioprotective effects of melatonin against XRI-induced skin damage is still lacking. In this investigation, we hypothesized that the melatonin can minimize the cell injury associated with XRI possibly through its antioxidant effects and DNA-repair effects. These effects would manifest as amelioration of the ultrastructural features of cell damage. To test our hypothesis and to fill this existing gap in the literature, we carried out this investigation. To accomplish our goals, we established an animal model consisting of nonirradiated, XRI and XRI-pretreated with melatonin. Our study clearly demonstrated that: (1) XRI is associated with ultrastructural features of both cell damage and increased metabolic activity and (2) melatonin can markedly minimize these changes.

XRI is associated with ultrastructural features of cellular damage

As compared to the nonirradiated skin, XRI skin showed features of cellular damage in the basal, spinous and granular cells. These features included destruction of the epidermal cells, decreased irregularity of the basal cell borders, swollen mitochondria, dilated RER, decreased complements of cytoplasmic organelles and loss of desmosomes. These ultrastructural features concur with previous studies (Tarpila 1971; Archambeau *et al*. 1984; Shirota & Tavassoli 1992; Enokihara *et al*. 1993; De Chatterjee *et al*. 1994; Landthaler *et al*. 1995; Yang *et al*. 1996; Shore *et al*. 2002). We propose that this tissue damage associated with XRI is due to the induction of the oxidative mechanisms. In turn, these mechanisms lead to an increase in malondialdehyde (MDA, an index of lipid peroxidation) and myeloperoxidase activity (MPO, an index of neutrophil infiltration) and the concomitant decrease in glutathione (GSH, a key to antioxidant).

Moreover, the irradiated cells displayed some early apoptotic changes such as reduction in the cytoplasmic and nuclear areas, extensive cytoplasmic vacuolization, abnormal ER, mitochondria and condensation of the nuclear chromatin. However, no apoptotic bodies were seen. These changes may reflect the upregulation of cell-cycle proteins such as p53. In turn, the latter can stimulate the apoptotic pathways inside the irradiated cells (Hussein *et al*. 2003b). We speculate that XRI can induce these early apoptotic changes by two possible mechanisms. First, XRI can induce the expression of proapoptotic Bcl-2 homology domains-3 only proteins, including Bcl-2-interacting domain; Bcl-X_L/Bcl-2-associated death promoter, and p53-upregulated modulator of apoptosis. These proteins can not only relay the death signals to the mitochondria, but also can facilitate the assembly of proapoptotic Bcl-2-associated X protein (Bax) and Bcl-2 antagonist killer 1 into the pores in the outer mitochondrial membrane. This process involves changes in mitochondrial permeability and release of various factors involved in apoptosis, including cytochrome *c* and apoptosis-inducing factor. The pro-apoptotic Bcl-2 proteins allow cytochrome *c* to leak out of the mitochondria. The released cytochrome *c* and apoptosis-activating factor-1 bind to caspase 9. Caspase 9 then activates the caspase cascade, leading to apoptotic cell death. Second, XRI can induce the expression of p53 protein which in turn forces the cells to commit apoptosis by modulating Bcl-2 and Bax genes' transcriptional activity (Hussein *et al*. 2003a, b).

XRI is associated with ultrastructural features of increased metabolic activity

As compared to the nonirradiated skin, XRI skin showed features of increased metabolic activity. These features included increased euchromatin, less density of the lipid droplets, irregularity of the nuclear membrane (indentations), hypertrophy and increased branching of the melanocytes.

Also, an increased number of the Birbeck granules was seen in the Langerhans cells. Of these features, the increased irregularity of the nuclear membrane is in keeping with similar findings in irradiated synovial intimal cells (Zichner & Engel 1971). This finding may be due to the presence of intracytoplasmic filaments (Bessis & Breton-Gorius 1965; Beltran & Stuckey 1972; Zucker-Franklin *et al*. 1974). These irregularities provide more areas of contact between the nucleus and the cytoplasm, i.e. nucleocytoplasmic exchange. The latter can enhance the metabolic activity of these cells (Love & Soriano 1971). The presence of relatively more euchromatin in the irradiated cells is suggestive of an enhanced metabolic activity following irradiation (Ghadially *et al*. 1985). The presence of chromatin margination and segregation in the irradiated cells is indicative of increased nuclear-cytoplasmic exchange, rapid growth and increased metabolism (Montironi *et al*. 1991a, b, c; Love & Soriano 1971; Ghadially *et al*. 1985; Teodori *et al*. 2000). Moreover, the presence of nucleolar margination in the irradiated cells is indicative of increased protein synthesis and nucleocytoplasmic exchange (Montironi *et al*. 1991a, b, c). This nucleolar segregation probably reflects DNA binding and inhibition of DNA-dependant RNA synthesis (Reddy & Svoboda 1968; Zatsepina *et al*. 1989). Also, the increase in the number of Birbecks granules may be due to increased synthetic and secretory activity of the Langerhans cells. This activity reflects change in the microenviroment (cytokines) following XRI (Roszkiewicz *et al*. 1990; Kohn *et al*. 2001).

In normal cells, hypertrophy of the mitochondria is indicative of enhanced metabolic activity. Alternatively, the paucity of mitochondria is indicative of predominance of anaerobic glycolysis relative to aerobic respiration in the cytoplasm and mitochondria, respectively. In this regard, the increased size of the mitochondria in the irradiated epidermal cells suggests that: (1) XRI results in increased metabolic activity in these cells; (2) the energy metabolism in these cells is still predominantly aerobic respiration rather than anaerobic glycolysis; and (3) these cells still have a differentiated phenotype.

Normally, the maturation of the melanosomes starts in the Golgi zone and proceeds to the cellular surface, i.e. orderliness. The previous studies indicated the absence of aberrant melanonosomes in the normal melanocytes. In keeping with these studies, melanosomes in the different stages of maturation were mixed together in the irradiated cells, indicating loss of orderliness (Jakubowicz *et al*. 1970; Cesarini 1971). Although, the underlying mechanisms for these changes are unclear, they may reflect deranged morphogenesis, with the melanin being deposited in a centrifugal fashion by the agency of vesicles (Konrad *et al*. 1974).

Melatonin can minimize the XRI skin damage

Our finding of ameliorated ultrastructural changes indicative of cellular damage in XRI skin pretreated with melatonin supports previous reports indicating radioprotective role of this substance (Undeger *et al*. 2004). In this regard, several experimental observations supported this radioprotective role. First, melatonin administration prior to irradiation prevented radiation damage on peripheral blood cells (Koc *et al*. 2002). Second, 6 and 8 Gy XRI of rats were associated with increased MDA, MPO, nitric oxide (NO) and decrease in GSH (Sener *et al*. 2003). All these indices were reduced with melatonin pretreatment (Taysi *et al*. 2003). Therefore, melatonin by its free radical scavenging and antioxidant properties ameliorates irradiation-induced organ injury (Sener *et al*. 2003). We propose that the ability of melatonin to ameliorate tissue damage may be due to its ability to enter cells and subcellular compartments easily, a feature not shared by most antioxidants (Reiter *et al*. 2003). Melatonin specifically enters the nucleus where it protects DNA from oxidative damage (Ressmeyer *et al*. 2003). Melatonin also improves cellular communication between normal and proliferating cells and alters the intracellular redox state (Reiter *et al*. 2003). Moreover, melatonin can ameliorate alterations in membrane fluidity and lipid peroxidation in microsomal membranes (Karbownik *et al*. 2000). The lack of signs of increased metabolic activity following XRI of the skin pretreated with melatonin supports previous reports indicating its oncostatic role (Undeger *et al*. 2004).

To summarize, to the best of our knowledge, this study is the first to report the ultrastructural changes following XRI in the skin. It also suggests radioprotective role for melatonin against XRI-induced skin damage. The presence of morphological changes following XRI supports the detrimental and possible carcinogenic effects of these rays. In this regard, further investigations are required to determine whether these XRI-induced ultrastructural changes reflect underlying DNA damage and genomic instability.

References

Archambeau J.O., Ines A. *et al*. (1984) Response of swine skin microvasculature to acute single exposures of X rays: quantification of endothelial changes. *Radiat. Res*. **98** (1), 37–51.

Beltran G. & Stuckey W.J. (1972) Nuclear lobulation and cytoplasmic fibrils in leukemic plasma cells. *Am. J. Clin. Pathol*. **58** (2), 159–164.

Berry R.J., Mole R.H. *et al*. (1976) Skin response to X-irradiation in the guinea-pig. *Int. J. Radiat Biol. Relat. Stud. Phys. Chem. Med*. **30** (6), 535–541.

Bessis M. & Breton-Gorius J. (1965) Role of the cytoplasm fibrils in lobulation of the cell nucleus (formation of Rieder's cells). *C R. Acad. Sci. Hebd. Seances Acad. Sci. D* **261** (5), 1392–1393.

Cesarini J.P. (1971) Recent advances in the ultrastructure of malignant melanoma. *Rev. Eur. Etud. Clin. Biol.* **16** (4), 316–322.

De Chatterjee J.K. *et al.* (1994) Low-level X-ray exposures on rat skin. Hyperkeratinization and concomitant changes in biometal concentration. *Biol. Trace Elem. Res.* **46** (3), 203–210.

Enokihara M.M., Pacheco I.P. *et al.* (1993) Ultrastructure of convoluted proximal tubule of kidney mice before and after X-ray exposure. *Rev. Paul. Med.* **111** (3), 403–406.

Ghadially F.N., Senoo A. *et al.* (1985) A serial section study of nuclear pockets containing nuclear material. *J. Submicrosc. Cytol.* **17** (4), 687–694.

Hickman A.B., Klein D.C. *et al.* (1999) Melatonin biosynthesis: the structure of serotonin N-acetyltransferase at 2.5 A resolution suggests a catalytic mechanism. *Mol. Cell.* **3**, 23–32.

Hussein M.R., Haemel A.K. *et al.* (2003a). Apoptosis and melanoma: molecular mechanisms. *J. Pathol.* **199** (3), 275–288.

Hussein M.R., Haemel A.K. *et al.* (2003b). p53-related pathways and the molecular pathogenesis of melanoma. *Eur. J. Cancer Prev.* **12** (2), 93–100.

Hussein M.R., Hassan M. *et al.* (2003c). Morphological changes and apoptosis in radial growth phase melanoma cell lines following ultraviolet-B irradiation. *Am. J. Dermatopathol.* **25**, 466–472.

Jakubowicz K., Dabrowski J. *et al.* (1970) Ultrastructure of melanosomes in malignant melanoma. *Dermatol. Monatsschr.* **156** (5), 299–307.

Karbownik M., Reiter R.J. *et al.* (2000) Protective effects of melatonin against oxidation of guanine bases in DNA and decreased microsomal membrane fluidity in rat liver induced by whole body ionizing radiation. *Mol. Cell Biochem.* **211**, 137–144.

Kim B.C., Shon B.S. *et al.* (2001) Melatonin reduces X-ray irradiation-induced oxidative damages in cultured human skin fibroblasts. *J. Dermatol. Sci.* **26**, 194–200.

Koc M., Buyukokuroglu M.E. *et al.* (2002) The effect of melatonin on peripheral blood cells during total body irradiation in rats. *Biol. Pharm. Bull.* **25**, 656–657.

Kohn D., Kohn S. *et al.* (2001) Birbeck granules in epidermal Langerhans cells of elderly patients with decubital ulcers. *Harefuah* **140** (8), 713–7, 806.

Konrad K., Honigsmann H. *et al.* (1974) Spilous nevus – a pigmented nevus with giant melanosoma. Clinical aspects, histology and ultrastructure. *Hautarzt* **25** (12), 585–593.

Landthaler M., Hagspiel H.J. *et al.* (1995) Late irradiation damage to the skin caused by soft X-ray radiation therapy of cutaneous tumors. *Arch. Dermatol.* **131** (2), 182–186.

Love R.& Soriano R.Z. (1971) Correlation of nucleolini with fine structural nucleolar constituents of cultured normal and neoplastic cells. *Cancer Res.* **31** (7), 1030–1037.

Montironi R., Braccischi A. *et al.* (1991a). Quantitation of the prostatic intra-epithelial neoplasia. Analysis of the nucleolar size, number and location. *Pathol. Res. Pract* **187** (2–3), 307–314.

Montironi R., Braccischi A. *et al.* (1991b). Value of quantitative nucleolar features in the preoperative cytological diagnosis of follicular neoplasias of the thyroid. *J. Clin. Pathol.* **44** (6), 509–514.

Montironi R., Scarpelli M. *et al.* (1991c). Quantitative analysis of nucleolar margination in diagnostic cytopathology. *Virchows Arch. A Pathol. Anat. Histopathol.* **419** (6), 505–512.

Reddy J. & Svoboda D. (1968) The relationship of nucleolar segregation to ribonucleic acid synthesis following the administration of selected hepatocarcinogens. *Lab. Invest.* **19** (1), 32–45.

Reiter R.J., Tan D.X. *et al.* (2003) Melatonin as an antioxidant: biochemical mechanisms and pathophysiological implications in humans. *Acta Biochim. Pol.* **50**, 1129–1146.

Ressmeyer A.R., Mayo J.C. *et al.* (2003) Antioxidant properties of the melatonin metabolite N1-acetyl-5-methoxykynuramine (AMK): scavenging of free radicals and prevention of protein destruction. *Redox Rep.* **8**, 205–213.

Roszkiewicz J., Roszkiewicz A. *et al.* (1990) Ultrastructural image of the Langerhans cells in the skin of patients with allergic contact dermatitis. *Przegl. Dermatol.* **77** (4), 241–248.

Sener G., Jahovic N. *et al.* (2003) Melatonin ameliorates ionizing radiation-induced oxidative organ damage in rats. *Life Sci.* **74**, 563–572.

Shirota T. & Tavassoli M. (1992) Alterations of bone marrow sinus endothelium induced by ionizing irradiation: implications in the homing of intravenously transplanted marrow cells. *Blood Cells* **18**, 197–214.

Shore R.E., Moseson M. *et al.* (2002) Skin cancer after X-ray treatment for scalp ringworm. *Radiat. Res.* **157** (4), 410–418.

Tarpila S. (1971) Morphological and functional response of human small intestine to ionizing irradiation. *Scand. J. Gastroenterol* **12**, 1–52.

Taysi S., Koc M. *et al.* (2003) Melatonin reduces lipid peroxidation and nitric oxide during irradiation-induced oxidative injury in the rat liver. *J. Pineal Res.* **34**, 173–177.

Teodori L., Tagliaferri F. *et al.* (2000) Selection, establishment and characterization of cell lines derived from a chemically-induced rat mammary heterogeneous tumor, by flow cytometry, transmission electron microscopy, and immunohistochemistry. *In Vitro Cell Dev. Biol. Anim.* **36** (3), 153–162.

Undeger U., Giray B. *et al.* (2004) Protective effects of melatonin on the ionizing radiation induced DNA damage in the rat brain. *Exp. Toxicol. Pathol.* **55**, 379–384.

Vijayalaxmi M.L., Meltz. *et al.* (1999a) Melatonin and protection from genetic damage in blood and bone marrow: whole-body irradiation studies in mice. *J. Pineal Res.* **27**, 221–225.

Vijayalaxmi M.L., Meltz. *et al.* (1999b) Melatonin and protection from whole-body irradiation: survival studies in mice. *Mutat. Res.* **425**, 21–27.

Vijayalaxmi R.L., Seaman *et al.* (1999c) Frequency of micronuclei in the blood and bone marrow cells of mice exposed to ultra-wideband electromagnetic radiation. *Int. J. Radiat. Biol.* **75**, 115–120.

Yang M.Q., Kjellen E. *et al.* (1996) The effect of ionizing irradiation on type I collagen of the tail in growing mice: a histology and electron microscopy study [Discussion]. *Scanning Microsc.* **10**, 821–831, 831–832.

Zatsepina O.V., Voronkova L.N. *et al.* (1989) Ultrastructural changes in nucleoli and fibrillar centers under the effect of local ultraviolet microbeam irradiation of interphase culture cells. *Exp. Cell Res.* **181** (1), 94–104.

Zichner L., Engel D. (1971) Electron microscopial examination of the ultra-sonic effect on the rabbit's synovial membrane. *Z. Gesamte Exp. Med.* **154** (1), 1–13.

Zucker-Franklin D., Melton J.W. III *et al.* (1974) Ultrastructural, immunologic, and functional studies on Sezary cells: aneoplastic variant of thymus-derived (T) lymphocytes. *Proc. Natl. Acad. Sci. USA* **71** (5), 1877–1881.